Differentiation and developmental pathways of uropathogenic *Escherichia coli* in urinary tract pathogenesis

Sheryl S. Justice*†, Chia Hung*†, Julie A. Theriot†‡, Daniel A. Fletcher§, Gregory G. Anderson*, Matthew J. Footer‡, and Scott J. Hultgren*¶

*Department of Molecular Microbiology, Box 8230, Washington University School of Medicine, 660 South Euclid Avenue, St. Louis, MO 63110; ‡Department of Biochemistry, Stanford University School of Medicine, Beckman Center, 279 West Campus Drive, Stanford, CA 94305; and §Department of Bioengineering, University of California, Berkeley, CA 94720

Communicated by M. J. Osborn, University of Connecticut Health Center, Farmington, CT, December 8, 2003 (received for review June 9, 2003)

Uropathogenic *Escherichia coli* (UPEC) are capable of forming complex intracellular bacterial communities (IBC) within the superficial umbrella cells of the bladders of C3H and BALB/c mice. By using time-lapse fluorescence videomicroscopy to observe infected mouse bladder explants, we discovered that IBCs formed by uropathogenic *E. coli* progressed through four distinct developmental stages that differed with respect to growth rate, bacterial length, colony organization, motility, and its eventual dispersal. In the first phase, bacteria in the IBC were nonmotile, rod shaped, and grew rapidly in loosely organized colonies free in the cytoplasm of the bladder superficial umbrella cells. In the second phase, the loose collection of bacteria in the IBC matured into a slower growing, highly organized biofilm-like community consisting of coccoid bacteria that ultimately filled most of the cytoplasm. In the third phase, bacteria in the biofilm-like state in the IBC switched to a motile rod-shaped phenotype allowing detachment from the community and eventual fluxing out of the host cell. During the fourth phase, the bacteria filamented. Filamentation appeared to be in response to a Toll-like receptor 4-mediated innate defense mechanism. Bacteria that fluxed out of the superficial umbrella cells were able to reenter the IBC developmental cascade but with slower kinetics and ultimately a quiescent reservoir was established. Intracellular growth and filamentation provided an advantage to the bacteria in evading infiltrating polymorphonuclear leukocytes. This work has developed a technique to observe live infected organs and revealed a complex differentiation pathway that facilitates bacterial persistence in the urinary tract.

Uropathogenic *Escherichia coli* (UPEC) are the major causative agent of urinary tract infections (UTIs) (1, 2). UTIs cause significant medical expenditures reaching $1.6 billion each year in the United States (1, 3). Clinically, UTIs are considered acute, self-limiting infections despite the prevalence of recurrent symptoms two or more times within months of a primary infection (1, 4). Several *in vitro* and *in vivo* models of infection have provided insights into the progression of UPEC-induced UTI (5–8). Type 1 pili on the bacterial surface recognize mannosylated proteins on the luminal surface of human and murine bladders (9–11), leading to binding and invasion into the superficial umbrella cells (7). In a murine model, it was shown that UPEC is able to replicate intracellularly, forming loose collections of bacteria termed "bacterial factories" (8). Bacteria within the superficial umbrella cells can escape into the bladder lumen in a process termed fluxing. Often, these fluxing bacteria are filamentous (8). The bladder epithelium responds to bacterial invasion via a Toll-like receptor 4 (TLR4) pathway that triggers the influx of polymorphonuclear leukocytes (PMNs) (5, 12). In addition, the superficial umbrella cells undergo an apoptosis-like cell death and exfoliate (6, 13), releasing bacteria into urine. Despite these strong host defenses, a subpopulation of UPEC is able to persist for months in our murine model in a quiescent reservoir state which may serve as a seed for recurrent infections (4, 6, 8, 14).

Recently, it was shown that *E. coli* strains NU14 and UTI89 formed intracellular bacterial biofilms within the cytoplasm of superficial umbrella cells of both C3H/HeN and C3H/HeJ mouse strains, creating a bulge on the bladder surface giving the appearance of a pod (15). Bacteria within the pod were incased in a polysaccharide-rich matrix and exhibited regional type 1 pili and antigen 43 immunoreactivity (15). These characteristics are similar to those found in biofilms on numerous surfaces in nature.

Although various pathogenic events have been well defined in several UTI models, snapshots of individual time points used to define these steps has not permitted their union into a timeline. Therefore, the sequence of events that leads to bacterial persistence and potential bacterial maturation events have been difficult to discern. Also, it was not known how growth rates might vary among the different bacterial morphological forms observed in fixed samples. Time-lapse videomicroscopy has been widely used to elucidate the sequence and timeline of dynamic events in host–pathogen interactions for tissue culture models of bacterial infections, but technical problems have limited its application to observe bacterial infections in intact primary tissues or organs. In this report, high-resolution time-lapse fluorescence videomicroscopy has been adapted to accommodate infected mouse bladder explants. Through this line of investigation, UTI89 was observed to progress through a multistage differentiation program while growing within the cytoplasm of superficial umbrella cells of the murine bladder. By combining transmitted light videomicroscopy with epifluorescence, an innate immune response characterized by infiltration of PMNs to phagocytose infecting UPEC could also be directly observed in real time and bacterial subversion mechanisms to these responses were discovered.

Materials and Methods

Bacterial Strains. UTI89 (8) was transformed with pCOMGFP (16). The bacteria were grown statically in LB containing 100 μg/ml carbenicillin for 24 h to induce the expression of type 1 pili.

Mouse Strains and Infections. Female BALB/c, C3H/HeN (The Jackson Laboratory) or C3H/HeJ (Harlan Breeding Laboratories) 8-week-old mice were inoculated with $\approx 2 \times 10^7$ bacteria by

Abbreviations: SEM, scanning electron microscopy; IBC, intracellular bacterial community; UPEC, uropathogenic *Escherichia coli*; UTI, urinary tract infection; PMN, polymorphonuclear leukocyte; r-WGA, tetramethylrhodamine-conjugated wheat germ agglutinin; TLR4, Toll-like receptor 4.

†S.S.J., C.H., and J.A.T. contributed equally to this work.

¶To whom correspondence should be addressed. E-mail: hultgren@borcim.wustl.edu.

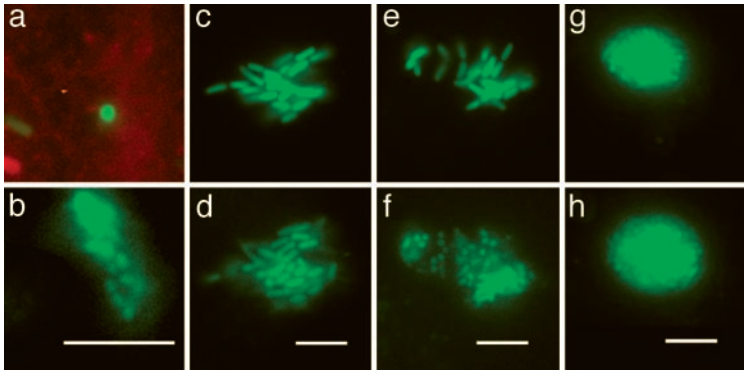

Fig. 1. Maturation of an IBC. These micrographs depict three stages of the developmental program of UPEC during the acute infection. GFP-producing bacteria were visualized by fluorescence videomicroscopy to monitor the events in real time by using r-WGA as a cell surface marker as described in the text. Each pair of micrographs depicts events observed in different superficial umbrella cells. Animated versions are available in Movies 1–3, which are published as supporting information on the PNAS web site. (*a*) At 2 h after infection, a single bacterium (green) is perpendicular to the bladder cell surface (red) and invades the cell over 10 min. (*b*) After 12 h, this bacterium formed an intracellular microcolony ≈2 μm below the surface. (*c* and *d*) The morphology and growth of the early IBC are depicted as snapshots taken 42 min apart. (*e* and *f*) Maturation to the middle IBC is depicted in snapshots taken 100 min apart. (*g* and *h*) Growth and architecture of the middle IBC are depicted as snapshots taken 42 min apart. (Scale bars = 10 μm.)

intraurethral catheterization as described (6). At 2- to 6-h intervals, the bladders were harvested, bisected, and splayed, and the luminal surface was stained with tetramethylrhodamine-conjugated wheat germ agglutinin (r-WGA) (Molecular Probes). Bladders harvested before 30 h after infection were pretreated with 100 μg/ml gentamicin sulfate (Sigma) for 30 min to kill extracellular bacteria at 37°C. Preliminary studies indicated that mouse bladder epithelium remained healthy, as determined by scanning electron microscopy (SEM), after overnight incubation in RPMI medium 1640/10% FCS in a humidified tissue culture incubator at 37°C (data not shown). With the exception of one bladder, results were obtained within 3 h after removal from the animals. The only exception was the bladder used in Fig. 1 *a* and *b*. This bladder remained in the incubated chamber for 12 h to evaluate the ability of the invading bacterium to support colony formation. Bladders were isolated every 4 h for the first 24 h after infection and every 6 h for the subsequent 24 h. To ensure validity of observed phenotypes, selected time points that overlap the previous time course were repeated. Portions of the bladders that were not used for videomicroscopy were fixed in 2.5% glutaraldehyde for 1 h and processed for visualization by SEM (17).

Time-Lapse Videomicroscopy. For imaging of live tissue, an anodized aluminum incubation chamber was constructed to immobilize and stretch the bladder tissue while mounted on the microscope stage (see Fig. 7, which is published as supporting information on the PNAS web site). A water channel drilled through the solid aluminum chamber enabled maintenance of temperature at 37°C by a circulating water bath. Four manual single-axis microtranslators with 4-mm travel range (Sutter Instruments, Novato, CA) were mounted on the chamber with cyanoacrylate adhesive. Tissue pins were mounted on each of the microtranslators. Pins were constructed by removing the stainless steel inserts from spinal tap needles, roughening the beveled ends with fine sandpaper, then cutting and bending so that the ends of the pins were separated by ≈1.5 mm in the center of the imaging chamber at a height such that the pins would put slight pressure on the coverslip at the bottom of the chamber when it was closed. Bladder tissue was trimmed to ≈2 mm^2, placed in the chamber with the luminal side facing down (toward the coverslip), and impaled with the four mounted pins. Tissue was stretched by slowly moving the pins apart with the microtranslators. After mounting, the chamber was filled with 5 ml of either RPMI medium 1640/10% FCS, or Hanks' buffered salt solution (HBSS) for viewing by videomicroscopy. HBSS was used instead of RPMI medium 1640/10% FCS at later times after infection to eliminate the potential effect of a rich medium on the growth and morphology of extracellular bacteria. A thin layer of silicone DC-200 oil (Fluka) was added to cover the surface of media in the chamber to prevent evaporation. Time-lapse imaging of infected explants was performed on a Nikon Diaphot-300 inverted microscope equipped with standard phase-contrast and epifluorescence optics, computer-controlled illumination shutters and filter wheels, and a back-thinned cooled charge coupled device digital camera (Princeton Instruments) using a PlanApo 60 × 1.4 numerical aperture Ph4 objective. Because tissue sample thickness precluded classical phase contrast imaging, a mismatched phase ring (Ph3) was selected on the long working distance condenser and aligned empirically to provide maximum contrast in the image. Individual bacteria could usually be identified by transmitted light as well as by GFP fluorescence, and the outlines of superficial umbrella cells and PMNs could be readily observed. Images were captured by using METAMORPH software (Universal Imaging, Media, PA). For most video sequences, pairs of transmitted light and epifluorescence images were collected at intervals of 3 s to 1 min. Paired images were collected within 1 s; image integration times were typically 100–400 msec. Measurements of distances were made by using NIH IMAGE (developed at the National Institutes of Health, http://rsb.info.nih.gov/nih-image).

Results and Discussion

UPEC utilizes complex mechanisms to subvert innate defenses to persist and cause disease. The ability of UPEC to invade into superficial cells of the bladder has been shown to be a critical mechanism in the ability of UPEC to establish a persistent infection (8, 12, 14, 15). Upon entry, UPEC diverts itself into the cytoplasm by an unknown mechanism that depends on the FimH adhesin present at the tips of type 1 pili (7). Previous light and electron microscopic studies identified loose intracellular collections of bacteria at early time points (≈6 h) in the superficial umbrella cells of the bladder, which were termed bacterial factories (8). In addition, at later time points (24 h) intracellular biofilm-like communities were observed that created a bulging appearance on the luminal surface of the bladder that were termed pods (15). Based on real-time fluorescence microscopy studies presented here, we discovered that these various structures are formed as part of a continuous developmental and

maturation cascade that UPEC undergoes while free in the cytoplasm. In addition, we discovered late maturation events that lead to dispersal of the intracellular bacterial community (IBC) subsequent to pod formation. All of the IBCs will be referred to as IBCs independent of their state of maturation or development to reflect the continuous maturation and development programs. Early, middle, and late IBCs were classified to delineate the distinct maturation stages and the unique community behaviors in each IBC.

Early IBCs. In a murine model, the binding and subsequent invasion of UPEC into the superficial umbrella cells on the luminal surface of the bladder are critical for the establishment of UTIs. In this study, invasion events were captured in real time (Fig. 1*a*) from 1 to 3 h after infection. After invasion, bacterial replication resulted in the formation of a loose collection of bacteria within the cytoplasm of the superficial umbrella cells ≈2–4 μm below the membrane surface (Fig. 1*b*). In the first 8 h of the IBC developmental program, the doubling times averaged between 30 and 35 min (Fig. 1 *c* and *d*) based on determining the length of time between septation events of randomly selected bacteria within the intracellular community. During this process, UPEC retained a rod shape (average length = 3 μm, SD = 0.8 μm), typical of that seen when grown under laboratory conditions, and the bacteria remained nonmotile in an amorphous clump (Fig. 1*c*). This rapid growth phase was observed up to 8 h after infection. The fast bacterial doubling time presumably facilitates a surge in the number of infectious organisms within the bladder, thus increasing the likelihood of persistence and dissemination.

Middle IBCs. Between 6 and 8 h after infection in both C3H/HeN and C3H/HeJ mice, the IBC underwent a series of dramatic maturation events leading to the formation of organized colonies with a number of specific biofilm-like traits (15). Each bacterium within the colony differentiated simultaneously (Fig. 1 *e* and *f* and Fig. 8, which is published as supporting information on the PNAS web site), suggesting that the maturation signal acted upon the entire population within the IBC. However, the molecular basis of these interbacterial communications have not yet been elucidated. A hallmark of the middle IBC was a reduction in average bacterial cell length (to 0.7 μm, SD, 0.2 μm) producing daughter cells that appeared coccoid in shape (Fig. 1*f*). The bacteria in the middle IBC at this point in the maturation program were more closely packed into tighter communities than in the early IBC. Individual septation events during middle IBC maturation were difficult to discern, but the doubling times were estimated to be >1 h based on the increase in the overall diameter of the IBC (Fig. 1 *g* and *h*). The maturation into the coccoid form did not coincide with nutrient depletion because continued growth of the middle IBC *in vivo* over a 10- to 14-h period resulted in bacterial occupation of almost the entire superficial umbrella cell. This stage of the infection coincides with the appearance of pods as described (15). A mature middle IBC consisted of a very dense and organized community with a globular architecture (Fig. 1*g*) within the cytoplasm of a superficial umbrella cell. These studies demonstrate that *E. coli* carry out a developmental differentiation cascade within superficial umbrella cells of the bladder whereby early IBCs mature from loose collections of bacteria into middle IBCs having a unique organized community with biofilm-like traits.

Late IBCs and Fluxing. As early as 12 h after infection, the coccoid bacteria on the outer edge of the middle IBC differentiated into the prototypical rod shape. Concurrently, the rod-shaped (average length = 2 μm, SD = 0.6 μm) bacteria became highly motile and dissociated from the IBC (Fig. 2 *a* and *b*). Motile

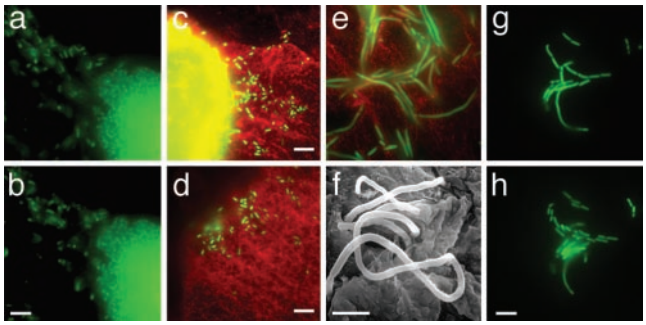

Fig. 2. Fluxing and filamentation. (*a* and *b*) Detachment and fluxing are depicted as snapshots taken 3 s apart. Detached bacteria are swimming rapidly. Animated versions are available in Movies 4 and 5, which are published as supporting information on the PNAS web site. (*c* and *d*) Two representative fluorescence micrographs depicting escaped bacteria (green) on the surface of two different superficial umbrella cells (red). The bright yellow patch (*c*) is the epifluorescence of the IBC within the superficial umbrella cell. Abundance of filamentous bacteria on the bladder surface is depicted by fluorescence micrograph (*e*) and by SEM (*f*). (*g* and *h*) The release of daughter cells from the filaments and their subsequent growth are depicted as snapshots taken 36 min apart. (Scale bars = 10 μm in *b–d* and *h* and 5 μm in *f*.)

bacteria were observed within superficial umbrella cells as well as fluxing out into the bladder lumen. Unlike the actin-based motility observed with other intracellular pathogens, the motility of intracellular and fluxed UPEC was characteristic of flagellar-based motility based on videomicroscopy. In all instances, motile bacteria exited the epithelial cells from a localized area on the epithelial cell surface. Fluxing into the lumen of the bladder presumably leads to bacteriuria (14) but, based on our video analysis, also facilitates the spread and colonization of other bladder cells (Fig. 2 *c* and *d*). Differentiation was not an artifact caused by exposure of the infected bladder to rich tissue culture medium because these same phenotypes were observed in bladders immediately upon harvesting and when the bladder was incubated in a buffered salt solution (HBSS). Late IBC eruption was highly unsynchronized leading to an apparent disparity in the timing of subsequent events. Although it is currently not known what environmental cues lead to fluxing, the fluxing event described here is highly similar to the "detachment" event that is described in biofilms formed on abiotic surfaces and may represent a change in the nutritional status of the late IBC. Because infected cells are undergoing apoptosis (6, 13), it is possible that the compromised cell membrane integrity may in part allow motile bacteria to escape. Furthermore, because the rate of exfoliation may vary from host to host, rapid exfoliation responses may preclude the ability of *E. coli* to complete the IBC maturation program.

UPEC Differentiates into a Filamentous Form *in Vivo*. Consistent with observations in previous studies, a subpopulation of the bacteria continued to grow but failed to septate, resulting in the formation of filamentous bacteria (8) (Fig. 2 *e* and *f*). Filamentous bacteria up to 70 μm in cell length (average length = 22 μm, SD = 14 μm) were first observed on the bladder surface ≈20 h after infection and were continually observed up to 48 h after infection. Although the differentiation into the filamentous form was not observed in real time, in some instances filamentous bacteria were observed on the edge of late IBCs with detaching bacteria, suggesting that filamentation may occur within the IBC. Alternatively, filamentation may occur on the bladder surface, and removal of the bladder may have abolished the conditions required for filamentation. Septation of filamentous bacteria on the bladder surface was observed, resulting in the release of rod-shaped daughters (4 μm ± 0.8 μm) (Fig. 2 *g* and *h*) that could

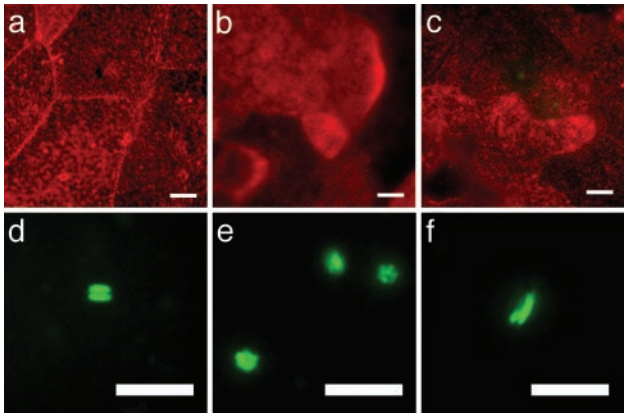

Fig. 3. Massive exfoliation and quiescent reservoir. (*a–c*) r-WGA staining of infected mouse bladder showed the presence of small, regenerating bladder epithelial cells after a massive exfoliation. (*d–f*) Fluorescence micrographs depicting bacteria within the superficial umbrella cells after exfoliation. The majority of the bacteria were pairs (*d*), small clusters (*e*), or a pair where one bacterium was longer than the other (*f*). (Scale bars = 10 μm.)

serve as a fresh population for invasion into other superficial umbrella cells or dissemination into the environment. Septation was observed while the bladder was incubated in HBSS without any nutritional source, suggesting that septation was not an artifact induced by rich medium. Differentiation into the filamentous form appeared to be a critical step for survival in the face of innate defenses as described below.

Cycling of the Developmental Cascade. Fluxing of bacteria and appearance of filaments coincided with the observation of small bacterial groups (usually pairs) within healthy superficial umbrella cells, consistent with a model in which fluxing leads to a second round of invasion and differentiation. The second-generation early IBCs had much longer doubling times ($\geq$60 min) but still progressed through the four phenotypes described above. All of the later stages of the developmental pathway also exhibited much slower growth rates. Therefore, in this system, the progression of UTIs involved at least two tandem rounds of infection and reinfection with an apparent adaptation to intracellular growth.

Bacterial Reservoir. The bladder epithelium undergoes exfoliation in response to bacterial infection (6, 13). r-WGA staining of the bladder surface 36–48 h after infection indicated that the majority of the bladder surface of both C3H/HeN and C3H/HeJ mouse strains consisted of superficial umbrella cells that were smaller than normal. (Fig. 3 *a–c*). In addition, many of these cells contained intracellular, rod-shaped bacteria in pairs, quadruplets, and small clusters that resembled those observed in the early stages of the second cycle of the pathogenic pathway (Fig. 3 *d–f*). Although no bacterial growth was detected, these bacteria continued the expression of GFP for at least 12 days after infection. Bladders examined at 4, 5, 6, and 12 days after infection, subsequent to establishment of reservoirs, showed no difference in the bacterial phenotype within the superficial umbrella cells. These clusters of quiescent bacteria may represent the reservoir as described (8, 12).

Evasion of PMN Attack. Mammalian hosts mount robust inflammatory responses in reaction to UTIs. PMNs are rapidly recruited to the bladder and play a major role in efficiently clearing extracellular bacteria (18). Starting $\approx$6 h after infection and continuing for an additional 32 h, PMNs directly navigated toward and swarmed onto infected superficial umbrella cells in the C3H/HeN but not the

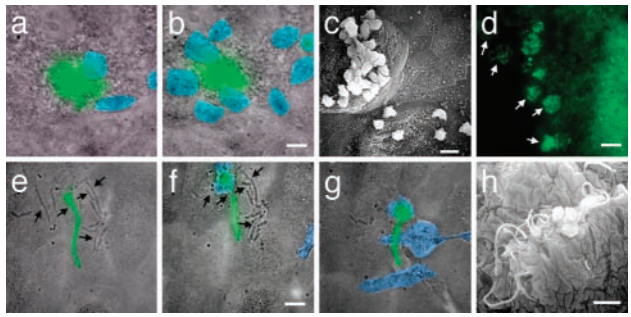

Fig. 4. Pod protects UPEC from PMN attack. Fluorescence micrographs were overlaid with a transmitted light image taken at the same time. The PMNs were pseudocolored blue for ease of visualization. Animated versions are available in Movies 6–9, which are published as supporting information on the PNAS web site. (*a*) From the surface, the epifluorescence of the IBC was observed (green) while PMNs (blue) swarm on the surface. (*b*) Ten minutes later, more PMNs have been recruited but fail to gain access to the IBC. (*c*) SEM of bladder surface showing the presence of numerous PMNs on the surface of infected cells but absent from uninfected cells. (*d*) Fluorescence micrograph depicting PMNs consuming the IBC (white arrows). (*e–g*) Overlay of the transmitted light image on the fluorescence micrograph depicting snapshots during which PMNs consume the dividing nonfluorescent bacteria (black arrows) but fail to consume the fluorescent filament. These frames were taken 13 min apart. (*h*) SEM of the bladder surface showing that filaments survive in the presence of PMNs. (Scale bars = 10 μm.)

C3H/HeJ mouse strain (Fig. 4 *a–c*). In contrast, swarming PMNs were not observed on noninfected superficial umbrella cells (Fig. 4*c*). This result illustrated that PMNs were highly efficient in discriminating infected from noninfected cells. Despite the numbers of PMNs around infected cells, the early and middle IBCs provided a safe haven for the intracellular bacteria to increase in number by delaying the ability of the PMNs to access and engulf the intracellular bacteria. Once PMNs gained access into an infected umbrella cell they would engorge themselves with bacteria (Fig. 4*d*), but were often unable to clear the entire bacterial population. Consequently, significant numbers of bacteria were able to escape PMN activity. These results demonstrated that the IBC developmental cascade provided a means to increase in number in the presence of the robust innate immune system to establish residency in the bladder and further disseminate into the environment.

Starting $\approx$20 h after infection, filamentous bacteria were the most abundant extracellular bacterial species observed on the bladder surface of C3H/HeN mice. The predominance of the filaments could result from a selection process because rod-shaped organisms were typically seen being eliminated by the PMNs. Filamentous bacteria appeared to survive the PMNs in two manners: (*i*) the PMNs did not respond to filamentous bacteria until initiation of septation; and (*ii*) the PMNs did not engulf the filamentous bacteria. In the cases where the PMNs appeared to be in direct contact with the filamentous bacteria, the bacteria were wrapped around the outside of the PMN, or were simply pushed

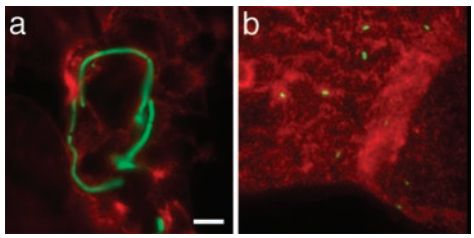

Fig. 5. Filamentation requires functional TLR-4. Filaments are observed on the luminal surface of the bladder from wild-type mice (C3H/HeN) (*a*) but are absent at the same time point in TLR-4-deficient mice (C3H/HeJ) (*b*).

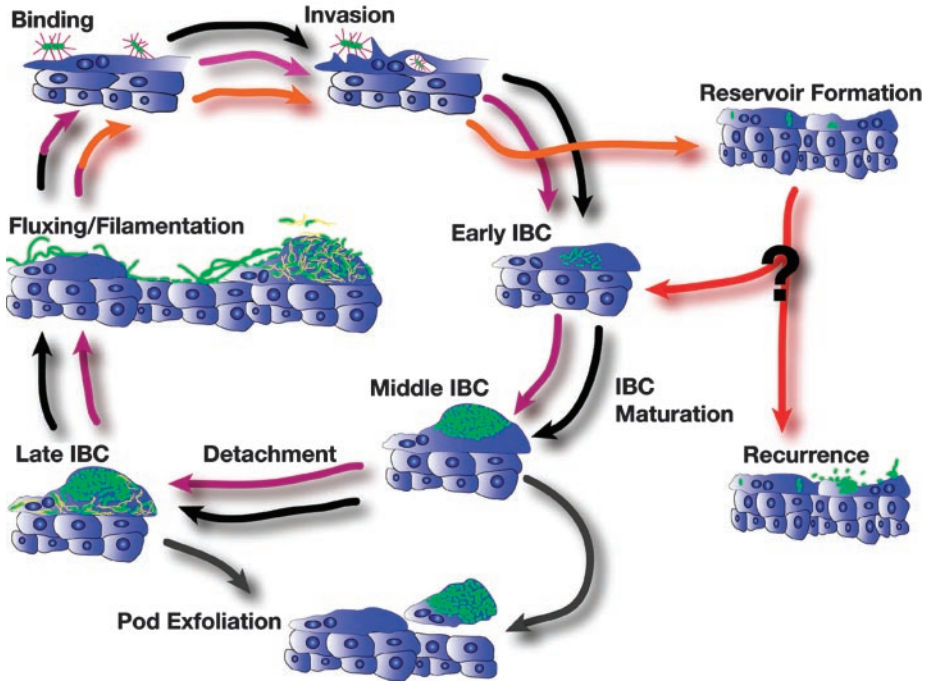

Fig. 6. UTI pathogenic cascade model. This model depicts the sequence of events during the progression of establishment of a UTI based on the data presented in this report in conjunction with previous studies. The first round of the developmental process (black arrows) directly leads to the second round (magenta arrows) that completes at the time of massive exfoliation of the superficial umbrella cells. At this time, the reservoir is established (orange arrows). Exfoliation of epithelial cells occurs as a mechanism of the innate immune system (gray arrows). Events that lead to recurrence and the mechanism of bacterial growth during recurrence are unclear (red arrows and question mark); these events may include reentry into the characterized cycle at the point of early IBC formation. Bacteria (green) bind to and invade into superficial umbrella cells via type 1 pili (purple). Detachment from IBC and fluxing out of infected cells likely involve flagella expression (yellow).

around the bladder surface by the movement of the PMNs (Fig. 4*h*) arguing that the PMNs were unable to kill the filamentous bacteria. Increased cell length is not sufficient to protect bacteria from PMN engulfment, as filaments produced by overproduction of the cell division inhibitor SulA are efficiently engulfed and killed by PMNs *in vitro* (S.S.J., D. A. Hunstad, and S.J.H., unpublished data). However, once septation resumed, the PMNs could readily phagocytose the newly born daughter cells but not other filamentous bacteria in the area (Fig. 4 *e–g*). Therefore, filamentation *in vivo* may provide the bacteria with an advantage to survive long enough to release daughters that either reinvade or disseminate into the environment.

Role of TLR-4 in Uropathogenesis. The experiments described above were performed in both C3H/HeN and C3H/HeJ mouse strains. C3H/HeJ mice have a mutation in *tlr-4*, rendering them hyporesponsive to lipopolysaccharide or Gram-negative bacteria (19). In general, the same bacterial developmental cycle occurred in both mouse strains, although temporal differences were observed. As predicted, PMNs were rarely observed during the entire progression of infection in the TLR-4-deficient mice. Of those observed, few contained fluorescent bacteria. Previous studies have shown that an acute inflammatory response is not mounted when the epithelial cells are deficient in TLR-4 even when hematopoietic cells were reconstituted with TLR-4-positive cells (20).

Host response is also involved in the induction of bacterial filamentation. Starting from 20 h after infection, the majority of bacteria on the bladder luminal surface in the C3H/HeN mice were filamentous, albeit some rod-shaped bacteria were also observed. In contrast, no filamentous bacteria were observed in the TLR-4-deficient mice (Fig. 5*b*) up to 48 h after induction. This observation suggests that a signal through the TLR-4 pathway directly or indirectly resulted in inhibition of septation. In response to bacterial infection, epithelial cells and immune cells produce a panel of cytokines, chemokines, and inflammatory molecules such as nitric oxide (5, 6, 12, 18, 21, 22). It is possible that filamentation is a consequence of bacterial stresses from either epithelial cells or PMN granule contents or both.

Concluding Remarks. Results presented in this study formulated a comprehensive model of UTI pathogenesis (Fig. 6). The developmental and maturation cascades of the IBCs played key roles in the ability to maximize infectious numbers and survive the host immune response. The exact timing of events described in this study is limited to the UPEC strain (UTI89) tested in C3H/HeN and C3H/HeJ mice. The same results were also observed in UTI89 infected BALB/c mice (S.S.J, C.H., J.A.T. and S.J.H., unpublished data) and early IBC formation and filamentous bacteria have been described using another cystitis UPEC strain, NU14, in various mouse strain combinations (6). The behavior of other UPEC and/or mouse strains is currently under investigation. This model will allow the testing of mutants to dissect out the key steps in the disease that could lead to the development of new antimicrobial agents in the treatment of UTIs.

We thank Mike Vieth for excellent technical help with SEM. We also thank Stanley Falkow, Matt Chapman, Karen Dodson, Yvonne Lee, and Steve Beverley for helpful discussions and Denise Monack for her invaluable assistance with the mice. This work was supported by National Institutes of Health Grants RO1AI48689, RO1AI29549, and R01DK51406, and Office of Research on Women's Health Specialized Center of Research P50DK64540 with the Food and Drug Administration (to S.J.H.), a Fellowship in Science and Engineering from the David and Lucile Packard Foundation (to J.A.T.), postdoctoral support from the Stanford Bio-X Program (to D.A.F.), and by an Individual National Research Service Award F32DK10168 (to S.S.J.).

1. Hooton, T. M. & Stamm, W. E. (1997) *Infect. Dis. Clin. N. Am.* **11,** 551–581.
2. Svanborg, C. & Godaly, G. (1997) *Infect. Dis. Clin. N. Am.* **11,** 513–529.
3. Foxman, B. (2002) *Am. J. Med.* **113,** Suppl 1A**,** 5S–13S.
4. Foxman, B. (1990) *Am. J. Public Health* **80,** 331–333.
5. Mysorekar, I. U., Mulvey, M. A., Hultgren, S. J. & Gordon, J. I. (2002) *J. Biol. Chem.* **277,** 7412–7419.
6. Mulvey, M. A., Lopez-Boado, Y. S., Wilson, C. L., Roth, R., Parks, W. C., Heuser, J. & Hultgren, S. J. (1998) *Science* **282,** 1494–1497.
7. Martinez, J. J., Mulvey, M. A., Schilling, J. D., Pinkner, J. S. & Hultgren, S. J. (2000) *EMBO J.* **19,** 2803–2812.
8. Mulvey, M. A., Schilling, J. D. & Hultgren, S. J. (2001) *Infect. Immun.* **69,** 4572–4579.
9. Hung, C.-S., Bouckaert, J., Hung, D., Pinkner, J., Widberg, C., De Fusco, A., Auguste, C. G., Strouse, B., Langerman, S., Waksman, G. & Hultgren, S. J. (2002) *Mol. Microbiol.* **44,** 903–915.
10. Jones, C. H., Pinkner, J. S., Roth, R., Heuser, J., Nicholes, A. V., Abraham, S. N. & Hultgren, S. J. (1995) *Proc. Natl. Acad. Sci. USA* **92,** 2081–2085.
11. McTaggart, L. A., Rigby, R. C. & Elliott, T. S. (1990) *J. Med. Microbiol.* **32,** 135–141.
12. Schilling, J. D., Mulvey, M. A., Vincent, C. D., Lorenz, R. G. & Hultgren, S. J. (2001) *J. Immunol.* **166,** 1148–1155.
13. Klumpp, D. J., Weiser, A. C., Sengupta, S., Forrestal, S. G., Batler, R. A. & Schaeffer, A. J. (2001) *Infect. Immun.* **69,** 6689–6695.
14. Schilling, J. D., Lorenz, R. G. & Hultgren, S. J. (2002) *Infect. Immun.* **70,** 7042–7049.
15. Anderson, G. G., Palermo, J. J., Schilling, J. D., Roth, R., Heuser, J. & Hultgren, S. J. (2003) *Science* **301,** 105–107.
16. Valdivia, R. H., Hromockyj, A. E., Monack, D., Ramakrishnan, L. & Falkow, S. (1996) *Gene* **173,** 47–52.
17. Kelly, R. O., Dekker, R. A. & Bluemink, J. G. (1973) *J. Ultrastruc. Res.* **45,** 254–258.
18. Haraoka, M., Hang, L., Frendeus, B., Godaly, G., Burdick, M., Strieter, R. & Svanborg, C. (1999) *J. Infect. Dis.* **180,** 1220–1229.
19. McAdam, K. P. & Ryan, J. L. (1978) *J. Immunol.* **120,** 249–253.
20. Schilling, J. D., Martin, S. M., Hung, C. S., Lorenz, R. G. & Hultgren, S. J. (2003) *Proc. Natl. Acad. Sci. USA* **100,** 4203–4208.
21. Svanborg, C., Godaly, G. & Hedlund, M. (1999) *Curr. Opin. Microbiol.* **2,** 99–105.
22. Poljakovic, M., Svensson, M. L., Svanborg, C., Johansson, K., Larsson, B. & Persson, K. (2001) *Kidney Int.* **59,** 893–904.